

## Magnetic field induced ferroelectricity and half magnetization plateau in polycrystalline $R_2V_2O_7$ ( $R = \text{Ni, Co}$ )

R. Chen,<sup>1</sup> J. F. Wang,<sup>1,\*</sup> Z. W. Ouyang,<sup>1,†</sup> Z. Z. He,<sup>2</sup> S. M. Wang,<sup>3</sup> L. Lin,<sup>3</sup> J. M. Liu,<sup>3</sup> C. L. Lu,<sup>1</sup> Y. Liu,<sup>4</sup> C. Dong,<sup>1,5</sup> C. B. Liu,<sup>1</sup> Z. C. Xia,<sup>1</sup> A. Matsuo,<sup>5</sup> Y. Kohama,<sup>5</sup> and K. Kindo<sup>5</sup>


<sup>1</sup>Wuhan National High Magnetic Field Center and School of Physics, Huazhong University of Science and Technology, Wuhan 430074, China

<sup>2</sup>State Key Laboratory of Structural Chemistry, Fujian Institute of Research on the Structure of Matter, Chinese Academy of Sciences, Fuzhou, Fujian 350002, China

<sup>3</sup>Laboratory of Solid State Microstructures and Innovative Center of Advanced Microstructures, Nanjing University, Nanjing 210093, China

<sup>4</sup>School of Physics and Technology, Wuhan University, Wuhan 430072, China

<sup>5</sup>The Institute for Solid State Physics (ISSP), University of Tokyo, Chiba 277-8581, Japan

 (Received 20 July 2018; revised manuscript received 28 September 2018; published 5 November 2018)

Low-dimensional frustrated antiferromagnet is a good model system to study exotic quantum physics. Here we report the observation of half magnetization plateau and ferroelectricity which emerge simultaneously in the bond-alternating skew-chain compounds  $R_2V_2O_7$  ( $R = \text{Ni, Co}$ ) induced by high magnetic fields. The half plateau is stabilized in fields of 8–30 T (7–12 T) for  $\text{Ni}_2\text{V}_2\text{O}_7$  ( $\text{Co}_2\text{V}_2\text{O}_7$ ), whereas two magnetic field induced ferroelectricities are located below and above this plateau. The remarkable high-field ferroelectricity for Ni or Co compound is about  $50\text{--}60 \mu\text{C}/\text{m}^2$  for the polycrystalline sample. The resulting magnetic field-temperature ( $H$ - $T$ ) phase diagrams are very complex and several distinct phase transitions are observed. The forced electric polarization by sweeping magnetic fields evidences a clear magnetoelectric coupling in  $\text{Co}_2\text{V}_2\text{O}_7$  associated with the low-field ferroelectricity. Our magnetization data also reveal that  $\text{Co}_2\text{V}_2\text{O}_7$  produces an effective spin-1/2 behavior at the magnetic ground state. These experimental findings improve the knowledge to multiferroics and pave the way for exploring the quantum state of frustrated antiferromagnets.

DOI: [10.1103/PhysRevB.98.184404](https://doi.org/10.1103/PhysRevB.98.184404)

### I. INTRODUCTION

Magnetization plateau and multiferroicity are two different emergent phenomena in frustrated antiferromagnets. The former describes a quantum state that the magnetization ( $M$ ) is magnetic field ( $H$ )-independent in a finite field range and its value is a fraction of saturation magnetization ( $M_s$ ) [1–4]. The latter refers to a phase where two or more ferroic orders such as antiferromagnetism and ferroelectricity coexist [5–7]. For instance, the observed 1/3 magnetization plateau in  $\text{Ba}_3\text{CoSb}_2\text{O}_9$  corresponds to a collinear “up-up-down” spin arrangement [2]; the spiral spin structure at a low temperature ( $T$ ) or under magnetic fields accounts for the magnetically driven ferroelectricity in  $\text{TbMnO}_3$  [5]. The materials which exhibit both magnetization plateau and multiferroicity are rare because of the strict requirement of their peculiar spin configurations. This kind of material is of particular interest and usually gives rise to a complex magnetic phase diagram. This has been studied, for instance, in the materials  $\text{CuFeO}_2$  and  $\text{Ni}_3\text{V}_2\text{O}_8$  [8–13]. Here we report two multiferroic materials  $R_2V_2O_7$  ( $R = \text{Ni, Co}$ ), in which ferroelectricity and half magnetization plateau were observed simultaneously in applied magnetic fields.

The vanadate compounds with a formula  $R_2V_2O_7$  ( $R = \text{Cu, Ni, Co, Mn}$ ) show a variety of crystallographic

geometries with different magnetic  $R^{2+}$  ions. The  $\text{Cu}_2\text{V}_2\text{O}_7$  compound crystallizes in at least three different polymorphs, namely,  $\alpha$ ,  $\beta$ , and  $\gamma$  phases with orthorhombic, monoclinic, and triclinic structures, respectively [14,15]. The compound  $\text{Mn}_2\text{V}_2\text{O}_7$  has distorted honeycomb layered structure and shows  $\alpha$  (triclinic) and  $\beta$  (monoclinic) phases in low and high-temperature regions [16], while  $\text{Ni}_2\text{V}_2\text{O}_7$  and  $\text{Co}_2\text{V}_2\text{O}_7$  stabilize in the ambient condition with a monoclinic structure [17,18]. Among all these materials,  $\alpha\text{-Cu}_2\text{V}_2\text{O}_7$  has attracted considerable attention due to its intriguing electronic and magnetic properties. This compound undergoes a canted antiferromagnetic ordering at  $T_C = 35 \text{ K}$  [19]. High magnetic field study reveals successive magnetic phase transitions and a complex  $H$ - $T$  phase diagram for  $H//a$  [20]. Interestingly, a giant electric polarization ( $P$ ) as large as  $0.55 \mu\text{C}/\text{cm}^2$  was observed below  $T_C$  [19]. Although the symmetric exchange striction, spin-dependent  $p$ - $d$  hybridization, etc. were proposed [19,21,22], the mechanisms of this magnetically driven ferroelectricity have not been well understood. Moreover,  $\alpha\text{-Cu}_2\text{V}_2\text{O}_7$  was regarded as the only multiferroic material among various  $R_2V_2O_7$  vanadate compounds [14].

Very recently, we studied  $\text{Ni}_2\text{V}_2\text{O}_7$  in pulsed magnetic fields up to 52 T and found that this compound also exhibits interesting magnetic phase transitions as  $\alpha\text{-Cu}_2\text{V}_2\text{O}_7$  [23]. The magnetic behavior of  $\text{Ni}_2\text{V}_2\text{O}_7$  is dominated by  $S = 1$   $\text{Ni}^{2+}$  ions. Figure 1 shows the two different  $\text{Ni}^{2+}$  sites in  $\text{Ni}_2\text{V}_2\text{O}_7$ . They form bond-alternating skew chains along the  $c$  axis and are separated by nonmagnetic tetrahedrons  $\text{VO}_4$  between the chains [17]. The previous study of magnetic

\*jfwang@hust.edu.cn

†zwouyang@hust.edu.cn

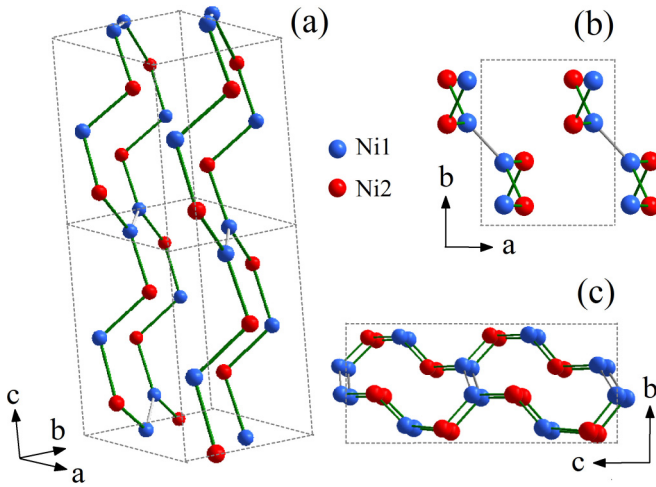


FIG. 1. Crystallographic geometry of  $\text{Ni}_2\text{V}_2\text{O}_7$ . (a) The two inequivalent  $\text{Ni}^{2+}$  ions (the blue and red symbols) showing the bond-alternating skew chains along the  $c$  axis.  $\text{Ni}_2\text{V}_2\text{O}_7$  crystallizes in a monoclinic structure with space group  $P2_1/c$ . (b), (c) The actual arrangements of  $\text{Ni}^{2+}$  ions viewed along the  $c$  and the  $a$  axis, respectively.

susceptibility and specific heat revealed magnetic transitions with a frustration of  $\theta_p/T_N = 4$ , where  $\theta_p$  is the Weiss constant and  $T_N$  is the magnetic ordering temperature [17]. Our high-field measurements revealed that a wide half magnetization plateau is stabilized in fields of 8–30 T, accompanied by an exotic nematiclike phase transition for magnetic fields applied along three crystallographic axes [23]. In the present work, we performed magnetization and electric polarization measurements on  $\text{Ni}_2\text{V}_2\text{O}_7$  and  $\text{Co}_2\text{V}_2\text{O}_7$  polycrystalline samples in magnetic fields up to 60 T. Our main findings include: (1) the analog  $\text{Co}_2\text{V}_2\text{O}_7$  with similar skew-chain structure shows a clear half magnetization plateau in 7–12 T and behaves as a low-spin ( $S = 1/2$ ) state at low temperature; (2) both compounds exhibit not only half magnetization plateau but also magnetically driven ferroelectricity ( $50\text{--}60 \mu\text{C}/\text{m}^2$ ); and (3) overall ferroelectric phase diagrams of the two compounds up to high magnetic fields. Therefore,  $\text{Ni}_2\text{V}_2\text{O}_7$  and  $\text{Co}_2\text{V}_2\text{O}_7$  are demonstrated to be a kind of multiferroic material exhibiting quantum effect. The magnetic phase transitions, the  $H$ - $T$  phase diagrams, as well as the magnetoelectric (ME) couplings of these two compounds were further investigated.

## II. EXPERIMENT

A comprehensive electric polarization study on a single crystal requires various measurements with magnetic fields and electrodes applied along different crystallographic axes. Due to the fact that the as-grown crystals are small and the crystal structure is monoclinic [23], it is difficult for us to measure electric polarization of  $\text{Ni}_2\text{V}_2\text{O}_7$  (or  $\text{Co}_2\text{V}_2\text{O}_7$ ) single crystals. Therefore, in this work we measured polycrystalline samples instead of single crystals, in a similar way as reported for  $\text{FeVO}_4$  [24]. This method helps for a rapid experimental preparation and to explore the magnetoelectric property in applied magnetic fields.  $\text{Ni}_2\text{V}_2\text{O}_7$  and  $\text{Co}_2\text{V}_2\text{O}_7$  polycrystalline samples were prepared using the conventional

solid-state reaction method. The resultant powders were pressed into pellets under 15 MPa and then sintered in air at  $500^\circ\text{C}$  for 48 h. The products were examined by x-ray powder diffraction (Philips X'Pert PRO). The magnetic susceptibility was measured by a commercial superconducting quantum interference device (SQUID). High-field magnetization was measured in pulsed fields using a coaxial pickup coil and calibrated by a comparison with the low-field data measured by SQUID. Polycrystalline samples with dimensions of  $5 \times 5 \times 0.3 \text{ mm}^3$  were used for electric polarization measurements. For the low-field dc measurement,  $P$  was measured by probing the zero-field pyroelectric current and isothermal polarized current via the Keithley 6514 electrometer connected with the Physical Property Measurement System (PPMS). The details can be found elsewhere [25]. For the pulsed high-field measurement, the pyroelectric current was detected by a shunt resistor ( $10 \text{ K}\Omega$ ) and  $P$  was derived from integrating the pyroelectric current with the time [13]. Different from the dc measurement, a bias field of  $E = 650 \text{ kV}/\text{m}$  was applied before and maintained during the short pulse ( $\sim 12 \text{ ms}$ ) to fully polarize the magnetic field induced ferroelectric (FE) domains in  $\text{R}_2\text{V}_2\text{O}_7$ .

## III. RESULTS AND DISCUSSION

Figure 2(a) shows the magnetic susceptibility ( $\chi = M/H$ ) of  $\text{Ni}_2\text{V}_2\text{O}_7$  measured in different magnetic fields. For  $H = 0.1 \text{ T}$ , two magnetic phase transitions are identified at low temperatures of  $T_1 = 6.9 \text{ K}$  and  $T_2 = 5.8 \text{ K}$ , which are in agreement with the specific-heat data reported for the

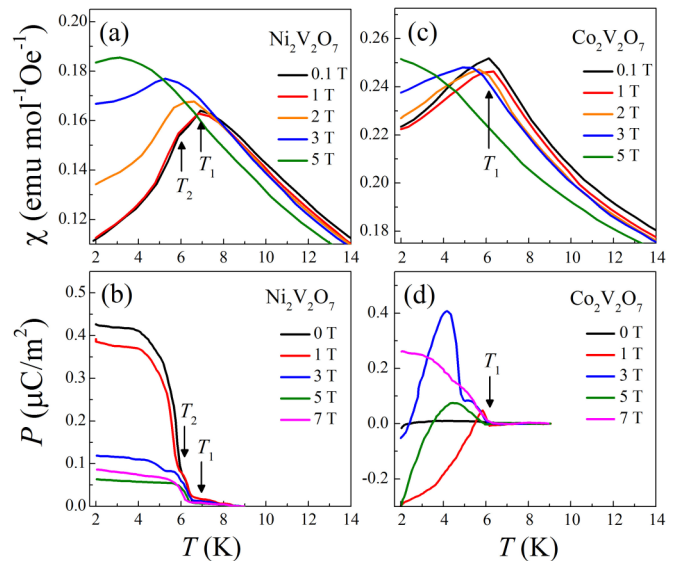


FIG. 2. (a)–(d) Temperature dependence of the magnetic susceptibility  $\chi$  and the electric polarization  $P$  of polycrystalline  $\text{Ni}_2\text{V}_2\text{O}_7$  and  $\text{Co}_2\text{V}_2\text{O}_7$  measured in various magnetic fields. For the  $P$  measurement, the sample was cooled down in a poling field ( $650 \text{ kV}/\text{m}$ ) through the transition temperature. This poling field was removed at the lowest temperature and the pyroelectric current was measured while warming at a constant rate of  $2 \text{ K}/\text{min}$ . The arrows indicate the transition temperatures of the magnetic and ferroelectric phase transitions.

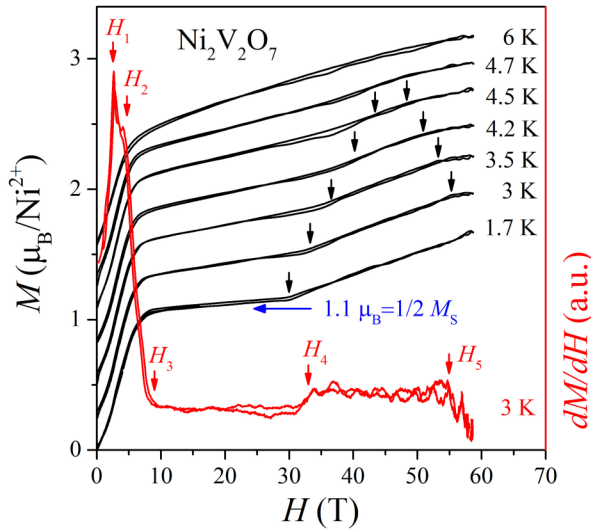


FIG. 3. The  $M(H)$  curve of polycrystalline  $\text{Ni}_2\text{V}_2\text{O}_7$  at various temperatures. The data for each temperature were vertically offset for clarity. The red curve denotes the derivative  $dM/dH$  at  $T = 3$  K. The arrows show the transition fields of  $H_1$ - $H_5$ .

$\text{Ni}_2\text{V}_2\text{O}_7$  single crystal [23]. The transition at  $T_1$  shows a change of slope in  $\chi$  indicating an antiferromagnetic ordering below this temperature. The transition at  $T_2$  is not clearly visible in  $\chi$  but is more easily noticed in the temperature derivative  $d\chi/dT$ . As  $H$  increases, these two transitions move to the low temperature and disappear above 3 T. Figure 2(b) shows the ferroelectric polarization  $P$  of  $\text{Ni}_2\text{V}_2\text{O}_7$  as a function of temperature. It is found that  $P$  is zero when  $T > T_1$  while it becomes nonzero ( $0.4 \mu\text{C}/\text{m}^2$  at 2 K) when  $T < T_1$ . As  $H$  increases,  $P$  is suppressed and preserved up to 7 T. The transition temperatures of  $P$  are slightly smaller than those determined by the susceptibility  $\chi$ . Similar results are obtained for the polycrystalline  $\text{Co}_2\text{V}_2\text{O}_7$  as shown in Figs. 2(c) and 2(d). Differently, only one transition temperature  $T_1$  is visible in  $\chi$ . In addition,  $P$  is almost zero at  $H = 0$  T but it is promoted by increasing  $H$ . These experimental results suggest that the emergence of ferroelectric polarization at the low temperature should arise from the origin of magnetism in these two compounds.

Figure 3 shows the  $H$  dependence of the magnetization of  $\text{Ni}_2\text{V}_2\text{O}_7$  in pulsed fields up to 60 T and in various temperatures. The derivative  $dM/dH$  at 3 K is also shown for a comparison. At 1.7 K, a clear magnetization plateau is stabilized in fields of 8–30 T as reported for the single crystal [23]. It is expected that the saturation value is  $2.2 \mu_{\text{B}}/\text{Ni}^{2+}$  with  $S = 1$  and  $g = 2.2$  [23]. Thus, the magnetization at this plateau ( $1.1 \mu_{\text{B}}/\text{Ni}^{2+}$ ) is exactly half of the saturation magnetization. Above 30 T,  $M$  increases linearly with  $H$  up to 60 T. Magnetic transitions of  $H_1$ - $H_4$  are clearly recognized at 2.5, 5, 9, and 29 T in the plot of  $dM/dH$ . Interestingly, when  $T$  is increased we observe another magnetic transition at  $H_5$  (55 T at 3 K) which was not detected in our previous study [23]. This transition moves to the low fields and converges with the transition of  $H_4$  at 4.7 K, where the half magnetization plateau almost disappears.

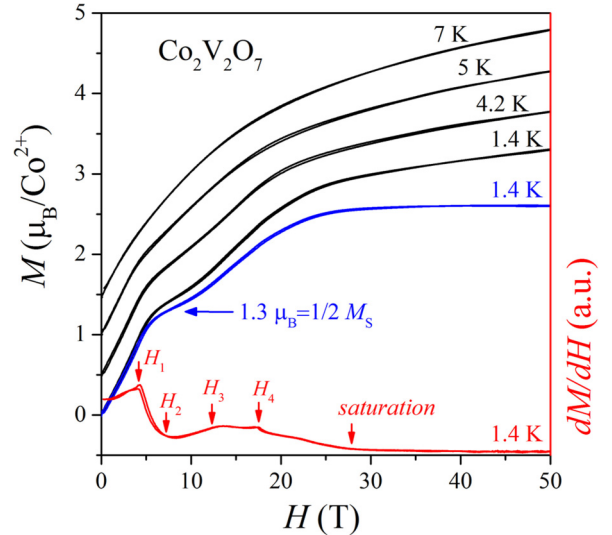


FIG. 4. High-field magnetization of polycrystalline  $\text{Co}_2\text{V}_2\text{O}_7$  at various temperatures. The  $M(H)$  curve was vertically offset for clarity. The red curve denotes the derivative  $dM/dH$  at  $T = 1.4$  K. The blue curve of 1.4 K is the result corrected for Van Vleck paramagnetism evaluated from the magnetization slope above the saturation field of 28 T. The arrows show the magnetic transitions at  $H_1$ - $H_4$  for  $dM/dH$ .

In order to verify the magnetization plateau in an analogous family compound, we measure the magnetization of polycrystalline  $\text{Co}_2\text{V}_2\text{O}_7$  in pulsed fields up to 50 T as shown in Fig. 4. Indeed, the magnetization process at 1.4 K shows a clear plateau in fields of 7–12 T, which vanishes when  $T$  is increased to 5 K. With increasing  $H$ , the magnetization nearly saturates above the critical field of 28 T. By extrapolating the  $M(H)$  curve above 28 T to a zero field, we subtract the Van Vleck paramagnetic susceptibility of the  $\text{Co}^{2+}$  ions. Corrected data are shown as the blue curve. It is found that the saturation magnetization is  $2.6 \mu_{\text{B}}/\text{Co}^{2+}$ , smaller than the expected value of  $3.87 \mu_{\text{B}}/\text{Co}^{2+}$  with  $S = 3/2$  and  $g = 2$ . This observation is reminiscent of the magnetic properties of  $\text{Ba}_3\text{CoM}_2\text{O}_9$  ( $M = \text{Sb}, \text{Ta}$ ), in which the  $\text{Co}^{2+}$  ions transfer from a high-spin ( $S = 3/2$ ) state at high temperature to a low-spin ( $S = 1/2$ ) state at the magnetic ground state [2,26]. From the saturation magnetization and the relation  $M_s = g\mu_{\text{B}}S$ , we estimate the Landé  $g$  factor to be 5.2 with  $S = 1/2$ . This large  $g$  factor implies that there exists a strong spin-orbit coupling in  $\text{Co}_2\text{V}_2\text{O}_7$  [18]. On the other hand, the explored plateau at 7–12 T is expectedly quantized at half of the saturation magnetization, as reported in  $\text{Ni}_2\text{V}_2\text{O}_7$ . In addition, magnetic transitions of  $H_1$ - $H_4$  are seen at 4, 7, 12, and 18 T in the derivative  $dM/dH$ . Note that the critical fields of the plateau and the saturation field are much smaller than those of  $\text{Ni}_2\text{V}_2\text{O}_7$ , indicating a relatively weak Co-Co exchange interaction in  $\text{Co}_2\text{V}_2\text{O}_7$ .

We further investigate the  $P$  variations of  $\text{Ni}_2\text{V}_2\text{O}_7$  and  $\text{Co}_2\text{V}_2\text{O}_7$  in pulsed fields up to 60 and 40 T, respectively. Figure 5(a) shows the data of  $\text{Ni}_2\text{V}_2\text{O}_7$  with magnetic fields applied parallel to the large surface of the sample, where the change of  $P$  is defined as  $\Delta P = P(H) - P(H = 0)$ . At low fields below  $H_2 = 5$  T,  $P$  slightly increases and then decreases



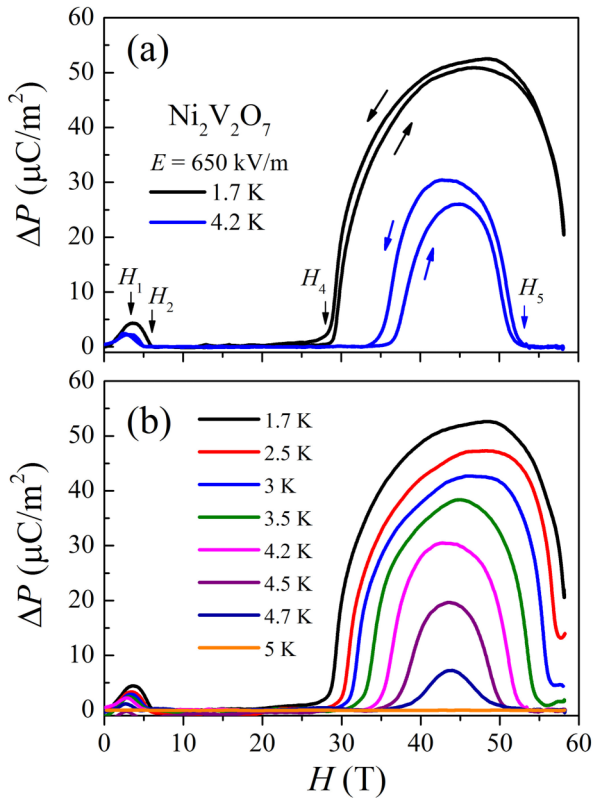


FIG. 5. The polarization  $P$  of polycrystalline  $\text{Ni}_2\text{V}_2\text{O}_7$  in fields up to 60 T. (a)  $P$  as a function of  $H$  measured at 1.7 and 4.2 K, respectively. Prior to the measurements, the sample was cooled down to 1.7 K (4.2 K) with zero poling field, then measurements were performed subsequently with a bias electric field of 650 kV/m during the pulse. The arrows indicate the field-rising (-falling) sweeps. (b)  $P$  measurements in various temperatures. Only the data in the falling sweeps are shown for clarity.

with a maximum at  $H_1 = 2.5$  T. When the magnetic field is further increased at 1.7 K,  $P$  is retained with nearly  $\Delta P = 0$  up to the critical field  $H_4 = 29$  T. The most striking feature of the high-field polarization is the big change of  $P$  above  $H_4$ , namely, magnetic field induced ferroelectricity. Remarkably, the maximum value of  $\Delta P$  above  $H_4$  is  $\sim 12$  times larger than that below  $H_2$ . In higher fields,  $\Delta P$  shows a sudden drop at 50 T and decreases toward zero up to 60 T. At 4.2 K, the high magnetic field can completely suppress  $P$  with  $\Delta P = 0$ . The corresponding transition field  $H_5$  is in agreement with that measured by the magnetization in Fig. 3. As  $T$  is increased, this high-field induced ferroelectricity develops well with  $T$  and finally vanishes above 5 K as shown in Fig. 5(b). Meanwhile, the low-field ferroelectricity also disappears at a higher temperature.

The polarization behavior of  $\text{Co}_2\text{V}_2\text{O}_7$  is shown in Fig. 6. Similar to  $\text{Ni}_2\text{V}_2\text{O}_7$ , two different  $H$ -induced ferroelectricities are observed in applied high magnetic fields. The  $\Delta P$  value reaches  $60 \mu\text{C}/\text{m}^2$  at 1.7 K and 15 T. As  $T$  is increased,  $\Delta P$  decreases gradually and disappears above 7 K. In comparison with  $\text{Ni}_2\text{V}_2\text{O}_7$ ,  $\text{Co}_2\text{V}_2\text{O}_7$  exhibits several distinct differences in the  $\Delta P(H)$  curve: (1) the low-field ferroelectricity centered at  $H_1$  has a larger  $\Delta P$  value of about  $50 \mu\text{C}/\text{m}^2$ ; (2) the

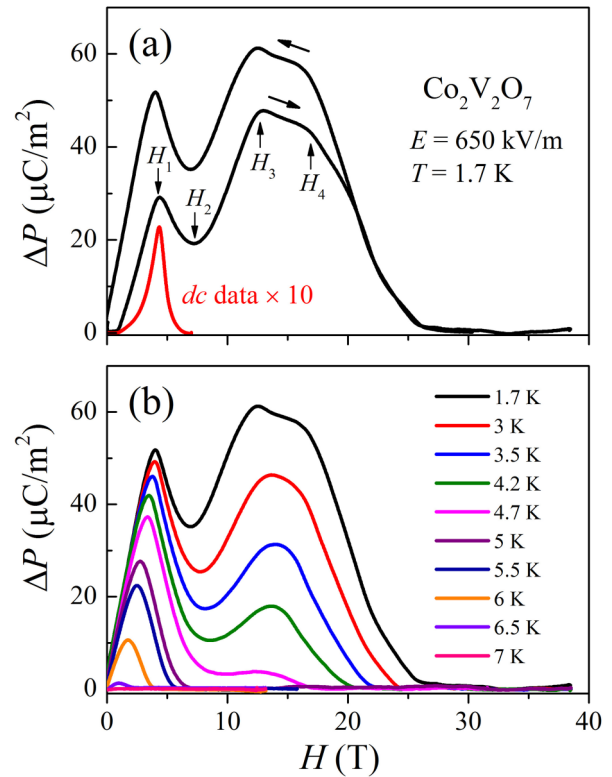


FIG. 6. The polarization  $P$  of polycrystalline  $\text{Co}_2\text{V}_2\text{O}_7$  in fields up to 40 T. (a)  $H$  variations of  $P$  measured at 1.7 K. The arrows indicate the field-rising (-falling) sweeps. We also show  $|\Delta P|$  versus  $H$  measured by a 7-T superconducting magnet for a comparison. Note that no bias electric field was applied during the 7-T measurement due to the limit of our equipment. (b)  $P$  measurements in temperatures from 1.7 to 7 K. Only the data in the falling sweeps are shown for clarity.

low-field and the high-field ferroelectricities move together, and the intermediate phase with  $\Delta P = 0$  is invisible; (3) the hysteresis of the  $H$ -induced ferroelectricities becomes larger; and (4) additional transitions can be seen in the high-field ferroelectricity in  $\text{Co}_2\text{V}_2\text{O}_7$ . To elucidate the low-field ferroelectricity and the intermediate phase around  $H_2$ , we measured the  $P$  variation in dc fields up to 7 T using the PPMS. The obtained  $P$  is small because the FE domains are not aligned under zero-bias electric field. Obviously, the evolutions of  $P$  in both dc and pulsed fields are similar and their transition fields are the same at  $H_1 = 4$  T. However, the dc data drop to zero at  $H_2$  where the magnetization plateau begins to appear. This feature is consistent with the result of  $\text{Ni}_2\text{V}_2\text{O}_7$  in Fig. 5. We speculate that in pulsed fields the nonzero  $\Delta P$  around  $H_2$  is attributed to the influence of leakage current in the  $\text{Co}_2\text{V}_2\text{O}_7$  sample. This may also lead to a big hysteresis for the  $H$ -decreasing sweep and a small remanent  $P$  at  $H = 0$ .

The  $H$ - $T$  phase diagrams determined from our magnetization and electric polarization measurements are summarized in Fig. 7. For  $\text{Ni}_2\text{V}_2\text{O}_7$  in Fig. 7(a), low- and high-field FE phases are well established through the magnetic phase transitions, indicating the nature of magnetically driven ferroelectricity. It is found that these two FE phases are separated by the half plateau and spin nematiclike phases for which the polarization is unchanged ( $\Delta P = 0$ ). In general, the magnetization

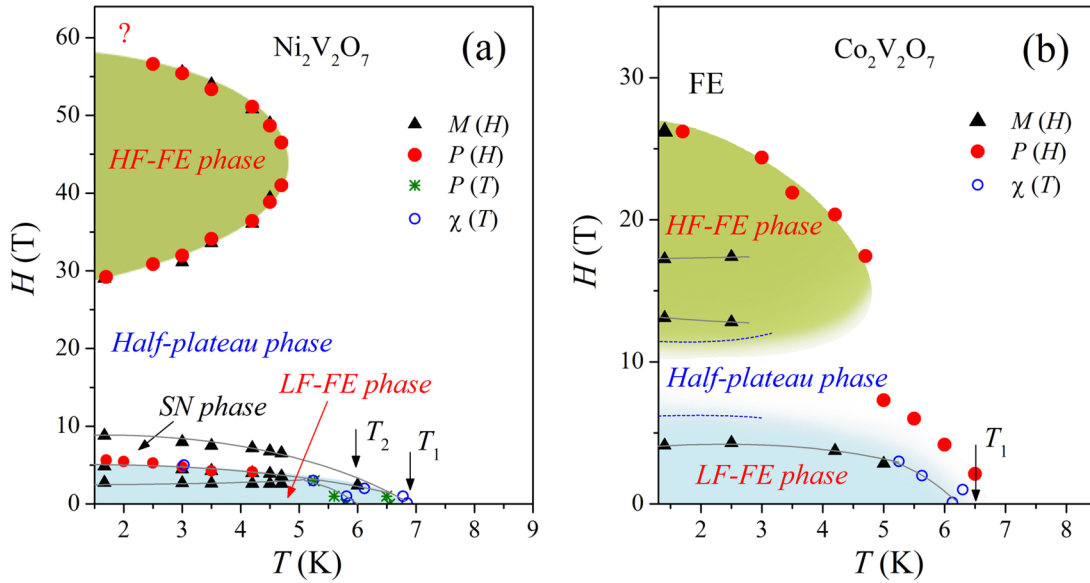


FIG. 7. High-field  $H$ - $T$  phase diagrams of (a)  $\text{Ni}_2\text{V}_2\text{O}_7$  and (b)  $\text{Co}_2\text{V}_2\text{O}_7$  determined from the magnetization, electrical polarization, and magnetic susceptibility measurements. The blue and the green areas denote the explored low-field (LF-FE) and high-field (HF-FE) ferroelectric phases, respectively. SN phase in Fig. 7(a) denotes the spin nematiclike phase. The thin solid lines are guides for the eyes. The dashed lines in Fig. 7(b) separate the FE phases and the half plateau phase in  $\text{Co}_2\text{V}_2\text{O}_7$  as proposed.

plateau has a collinear commensurate spin configuration [2], while the spin-dependent ferroelectricity is incommensurate helical (or spiral) spin ordered [6]. This scenario has already been observed in the materials  $\text{CuFeO}_2$  and  $\text{Ni}_3\text{V}_2\text{O}_8$  where the plateau and the FE phases are well separated [9,13]. Thus, it is reasonable that a half magnetization plateau will yield a paraelectric state ( $P = 0$ ) in the frustrated magnet  $\text{Ni}_2\text{V}_2\text{O}_7$  or  $\text{Co}_2\text{V}_2\text{O}_7$ . Based on these results, we propose the phase diagram of  $\text{Co}_2\text{V}_2\text{O}_7$  in Fig. 7(b), although our present experiment cannot give a clear phase boundary between the half plateau and the high-field FE phase (Fig. 6).

Compared with  $\text{Co}_2\text{V}_2\text{O}_7$ , the phase diagram of  $\text{Ni}_2\text{V}_2\text{O}_7$  looks more complex in the low-field region. A spin nematiclike phase with  $\Delta P = 0$  is manifest before the system goes into the plateau phase, while no analogical phase is visible for  $\text{Co}_2\text{V}_2\text{O}_7$ . One reason is that  $\text{Co}_2\text{V}_2\text{O}_7$  perhaps has a strong magnetic anisotropy which makes the corresponding phase boundaries and the half plateau smeared because of the polycrystalline sample. Another reason may be ascribed to the different magnetic structures of these two compounds at low temperatures. For  $\text{Co}_2\text{V}_2\text{O}_7$ , only one magnetic transition is seen at  $T_1$  and the magnetization increases linearly in a low field (Fig. 4). In contrast,  $\text{Ni}_2\text{V}_2\text{O}_7$  undergoes two successive magnetic orderings at  $T_1$  and  $T_2$ . In a magnetic field, a spin-flop transition and a strong inflection take place followed by a linear increase of  $M$  near the plateau [23], also see Fig. 3 in this work. These behaviors are consistent with those features observed in  $\text{LiCuVO}_4$  which is a candidate to realize the spin nematic phase [27–29]. In this sense, it is likely that  $\text{Ni}_2\text{V}_2\text{O}_7$  has a more complicated spiral spin structure than that of  $\text{Co}_2\text{V}_2\text{O}_7$  in the magnetized ground state. This may also result in a much smaller  $P$  value ( $\sim 5 \mu\text{C}/\text{m}^2$ ) of the low-field FE phase than that ( $\sim 50 \mu\text{C}/\text{m}^2$ ) of  $\text{Co}_2\text{V}_2\text{O}_7$ . On the other hand, our experiments reveal that high magnetic fields can completely suppress the spiral spin arrangement by realization

of the half magnetization plateau. In addition, sufficient high fields can reorient the spin arrangement to spiral structure and lead to an enhanced  $P$  of the high-field FE phase. Consequently, two distinct ferroelectric phases exist linked by the half magnetization plateau phase for both compounds.

The appearance of the high-field FE phase is quite interesting. Especially for  $\text{Ni}_2\text{V}_2\text{O}_7$ , the change of  $M$  above  $H_4$  is smaller than that below  $H_2$  (Fig. 3), whereas  $\Delta P$  of the high-field phase is much larger than that of the low-field one (Fig. 5). Emergence of the FE phase after closing a gap (end of the plateau in this work) reminds us of the ferroelectricity in the quantum magnet  $\text{TlCuCl}_3$  [30]. In this material, mixture of the singlet and triplet states causes nonzero matrix element of  $\langle S_i \times S_j \rangle$ , which results in finite electric polarization in the Bose-Einstein condensation region. It would be interesting if there exists a similar quantum state in the field-temperature region of  $\text{Ni}_2\text{V}_2\text{O}_7$  (or  $\text{Co}_2\text{V}_2\text{O}_7$ ). Nevertheless, for  $\text{Ni}_2\text{V}_2\text{O}_7$ , the closure of this FE phase at  $\sim 58$  T is puzzling because the expected saturation field is  $\sim 80$  T according to our previous study [23]. It seems that this departure of the transition field cannot be understood by the anisotropy of the  $H$ - $T$  phase diagrams of  $\text{Ni}_2\text{V}_2\text{O}_7$ . With respect to  $\text{Co}_2\text{V}_2\text{O}_7$ , the saturation field corresponds to the ferroelectric-to-paraelectric phase transition. We suppose that the high-field FE phase of  $\text{Ni}_2\text{V}_2\text{O}_7$  is likely not a simple canted ferromagnetic phase and may collapse before reaching the saturation field, leading to a transition at  $\sim 58$  T to another spin-ordered phase like umbrella type.

Finally, the magnetoelectric responses of the above two samples were investigated. Note that this effect is associated with the low-field FE phase. For  $\text{Ni}_2\text{V}_2\text{O}_7$ , it may exist but the small  $P$  is out of the sensitivity limit of the instrument. For  $\text{Co}_2\text{V}_2\text{O}_7$ , the experimental result is shown in Fig. 8 due to a relatively large  $P$  with  $H$  increasing. It is seen that the ME response begins from the negative magnetic fields after the

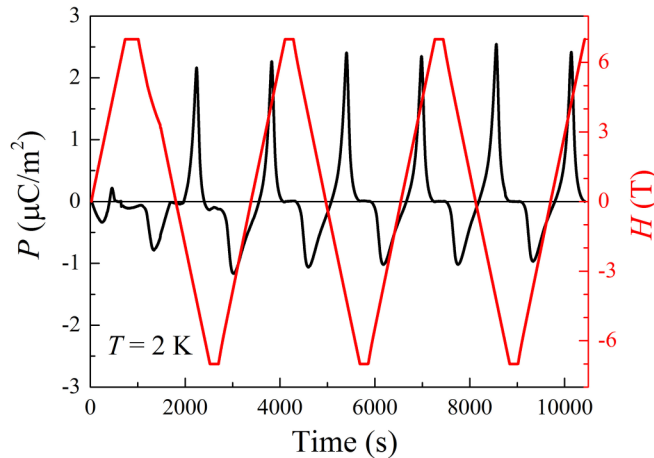


FIG. 8. Time dependence of the forced electric polarization of  $\text{Co}_2\text{V}_2\text{O}_7$  (left scale) with simultaneous magnetic field change (right scale) measured at 2 K. This measurement was performed by the PPMS with zero electric field. The oscillation of the magnetic field reaches the maximum of  $\pm 7$  T of the instrument.

activation of frozen FE domain wall by  $H$  sweeping [10]. The fact that  $P$  has a maximum (or minimum) value at  $\pm 4$  T and returns to zero at  $\pm 7$  T is in agreement with the  $\Delta P(H)$  data in Fig. 6(a). Particularly, the reversal of  $P$  with the maximum change of about  $3.4 \mu\text{C}/\text{m}^2$  can be directly manipulated by the continuous sweep field up to  $\pm 7$  T. The frequency of  $P$  is a double of that of  $H$ , in agreement with that observed in  $\text{FeVO}_4$  [24]. This result demonstrates the existence of a clear ME coupling between magnetic and ferroelectric orders in this material.

It should be pointed out that the present observation of half magnetization plateaus in polycrystalline samples is indeed inconsistent with that in a honeycomb spin system  $\text{Ba}_2\text{CoTeO}_6$ .  $\text{Ni}_2\text{V}_2\text{O}_7$  shows an isotropic feature of the half plateau for  $H$  applied along all crystallographic axes [23],

while the half plateau in  $\text{Ba}_2\text{CoTeO}_6$  is anisotropic and appears only for  $H$  applied along the  $c$  axis [31]. This inconsistency infers that  $\text{Ni}_2\text{V}_2\text{O}_7$  can be described with a different spin structure of  $\text{Ba}_2\text{CoTeO}_6$ , and this may arise from the ME coupling that exists in this material.

#### IV. CONCLUSION

The magnetic and dielectric properties of polycrystalline  $\text{R}_2\text{V}_2\text{O}_7$  ( $R = \text{Ni}, \text{Co}$ ) have been investigated in high magnetic fields up to 60 T. Half magnetization plateau and magnetic field induced ferroelectricities were observed simultaneously in both compounds. The resulting high-field phase diagrams are very complex in which the half plateau phases and the ferroelectric phases are well separated. In addition, an intriguing magnetoelectric coupling has been demonstrated for  $\text{Co}_2\text{V}_2\text{O}_7$  with the low magnetic field driven ferroelectricity. The high magnetic field driven ferroelectricity for Ni or Co compound is about  $50\text{--}60 \mu\text{C}/\text{m}^2$ . It is worth mentioning that our polarization measurements were performed on the polycrystalline samples. Detailed investigations based on large-sized single crystals are desirable in order to clarify the mechanisms of the magnetically driven ferroelectricities and the quantized magnetization plateau in these fascinating materials.

#### ACKNOWLEDGMENTS

J.F.W. would like to thank M. Tokunaga for useful comments about the high-field electric polarization results. This work was supported by the National Natural Science Foundation of China (Grants No. 11574098, No. U1832214, No. 11474110, and No. 51571152) and the National Key R&D Program of China (Grant No. 2016YFA0401704). J.M.L. acknowledges support from The National Key Research Project of China (Grant No. 2016YFA0300101) and NSFC (Grant No. 51721001).

- 
- [1] M. Oshikawa, M. Yamanaka, and I. Affleck, *Phys. Rev. Lett.* **78**, 1984 (1997).
- [2] Y. Shirata, H. Tanaka, A. Matsuo, and K. Kindo, *Phys. Rev. Lett.* **108**, 057205 (2012).
- [3] M. Jaime, R. Daou, S. A. Crooker, F. Weickert, A. Uchida, A. E. Feiguin, C. D. Batista, H. A. Dabkowska, and B. D. Gaulin, *Proc. Natl. Acad. Sci. USA* **109**, 12404 (2012).
- [4] H. Ishikawa, M. Yoshida, K. Nawa, M. Jeong, S. Kramer, M. Horvatic, C. Berthier, M. Takigawa, M. Akaki, A. Miyake, M. Tokunaga, K. Kindo, J. Yamaura, Y. Okamoto, and Z. Hiroi, *Phys. Rev. Lett.* **114**, 227202 (2015).
- [5] T. Kimura, T. Goto, H. Shintani, K. Ishizaka, T. Arima, and Y. Tokura, *Nature (London)* **426**, 55 (2003).
- [6] T. Yoshinori, S. Shinichiro, and N. Naoto, *Rep. Prog. Phys.* **77**, 076501 (2014).
- [7] S. Dong, J.-M. Liu, S.-W. Cheong, and Z. Ren, *Adv. Phys.* **64**, 519 (2015).
- [8] N. Terada, Y. Narumi, K. Katsumata, T. Yamamoto, U. Staub, K. Kindo, M. Hagiwara, Y. Tanaka, A. Kikkawa, H. Toyokawa, T. Fukui, R. Kanmuri, T. Ishikawa, and H. Kitamura, *Phys. Rev. B* **74**, 180404 (2006); N. Terada, Y. Narumi, Y. Sawai, K. Katsumata, U. Staub, Y. Tanaka, A. Kikkawa, T. Fukui, K. Kindo, T. Yamamoto, R. Kanmuri, M. Hagiwara, H. Toyokawa, T. Ishikawa, and H. Kitamura, *ibid.* **75**, 224411 (2007).
- [9] T. Kimura, J. C. Lashley, and A. P. Ramirez, *Phys. Rev. B* **73**, 220401 (2006).
- [10] H. Tamatsukuri, S. Mitsuda, T. Nakajima, K. Shibata, C. Kaneko, K. Takehana, Y. Imanaka, N. Terada, H. Kitazawa, K. Prokes, S. Matas, K. Kiefer, S. Paecel, A. Sokolowski, B. Klemke, and S. Gerischer, *Phys. Rev. B* **93**, 174101 (2016); J. Beilsten-Edmands, S. J. Magorrian, F. R. Foronda, D. Prabhakaran, P. G. Radaelli, and R. D. Johnson, *ibid.* **94**, 144411 (2016).
- [11] G. Lawes, A. B. Harris, T. Kimura, N. Rogado, R. J. Cava, A. Aharony, O. Entin-Wohlman, T. Yildirim, M. Kenzelmann, C. Broholm, and A. P. Ramirez, *Phys. Rev. Lett.* **95**, 087205 (2005).
- [12] J. F. Wang, M. Tokunaga, Z. Z. He, J. I. Yamaura, A. Matsuo, and K. Kindo, *Phys. Rev. B* **84**, 220407 (2011).

- [13] Y. J. Liu, J. F. Wang, Z. Z. He, C. L. Lu, Z. C. Xia, Z. W. Ouyang, C. B. Liu, R. Chen, A. Matsuo, Y. Kohama, K. Kindo, and M. Tokunaga, *Phys. Rev. B* **97**, 174429 (2018).
- [14] S. Bhowal, J. Sannigrahi, S. Majumdar, and I. Dasgupta, *Phys. Rev. B* **95**, 075110 (2017).
- [15] Z. Z. He and Y. Ueda, *Phys. Rev. B* **77**, 052402 (2008).
- [16] Z. Z. He and Y. Ueda, *J. Cryst. Growth* **310**, 171 (2008); *J. Solid State Chem.* **181**, 235 (2008); Z. Z. He, Y. Ueda, and M. Itoh, *Solid State Commun.* **147**, 138 (2008).
- [17] Z. Z. He, J. I. Yamaura, Y. Ueda, and W. Cheng, *Phys. Rev. B* **79**, 092404 (2009).
- [18] Z. Z. He, J. I. Yamaura, Y. Ueda, and W. Cheng, *J. Solid State Chem.* **182**, 2526 (2009).
- [19] J. Sannigrahi, S. Bhowal, S. Giri, S. Majumdar, and I. Dasgupta, *Phys. Rev. B* **91**, 220407 (2015).
- [20] G. Gitgeatpong, M. Suewattana, S. Zhang, A. Miyake, M. Tokunaga, P. Chanlert, N. Kurita, H. Tanaka, T. J. Sato, Y. Zhao, and K. Matan, *Phys. Rev. B* **95**, 245119 (2017).
- [21] Y. W. Lee, T. H. Jang, S. E. Dissanayake, L. Seunghun, and H. J. Yoon, *Europhys. Lett.* **113**, 27007 (2016).
- [22] J. T. Zhang, J. L. Wang, C. Ji, B. X. Guo, W. S. Xia, X. M. Lu, and J. S. Zhu, *Phys. Rev. B* **96**, 165132 (2017).
- [23] Z. W. Ouyang, Y. C. Sun, J. F. Wang, X. Y. Yue, R. Chen, Z. X. Wang, Z. Z. He, Z. C. Xia, Y. Liu, and G. H. Rao, *Phys. Rev. B* **97**, 144406 (2018).
- [24] B. Kundys, C. Martin, and C. Simon, *Phys. Rev. B* **80**, 172103 (2009).
- [25] M. F. Liu, H. M. Zhang, X. huang, C. Y. Ma, S. Dong, and J. M. Liu, *Inorg. Chem.* **55**, 2709 (2016).
- [26] K. M. Ranjith, K. Brinda, U. Arjun, N. G. Hegde, and R. Nath, *J. Phys.: Condens. Matter* **29**, 115804 (2017).
- [27] L. E. Svistov, T. Fujita, H. Yamaguchi, S. Kimura, K. Omura, A. Prokofiev, A. I. Smirnov, Z. Honda, and M. Hagiwara, *JETP Lett.* **93**, 21 (2011).
- [28] N. Buttgen, K. Nawa, T. Fujita, M. Hagiwara, P. Kuhns, A. Prokofiev, A. P. Reyes, L. E. Svistov, K. Yoshimura, and M. Takigawa, *Phys. Rev. B* **90**, 134401 (2014).
- [29] A. Orlova, E. L. Green, J. M. Law, D. I. Gorbunov, G. Chanda, S. Krämer, M. Horvatic, R. K. Kremer, J. Wosnitza, and G. L. J. A. Rikken, *Phys. Rev. Lett.* **118**, 247201 (2017).
- [30] S. Kimura, K. Kakihata, Y. Sawada, K. Watanabe, M. Matsumoto, M. Hagiwara, and H. Tanaka, *Nat. Commun.* **7**, 12822 (2016).
- [31] P. Chanlert, N. Kurita, H. Tanaka, D. Goto, A. Matsuo, and K. Kindo, *Phys. Rev. B* **93**, 094420 (2016).